IEEE Access
Multidisciplinary | Rapid Review | Open Access Journal

Received March 14, 2021, accepted April 5, 2021, date of publication April 20, 2021, date of current version May 7, 2021.

Digital Object Identifier 10.1109/ACCESS.2021.3072058

An Improved Intelligent Driver Model Considering the Information of Multiple Front and Rear Vehicles

FANG ZONG[1], MENG WANG[1], MING TANG[1], XIYING LI[2], AND MENG ZENG[1]
[1]College of Transportation, Jilin University, Changchun 130000, China
[2]School of Intelligent Systems Engineering, Sun Yat-sen University, Guangzhou 510275, China

Corresponding authors: Meng Zeng (zengmeng18@mails.jlu.edu.cn) and Xiying Li (stslxy@mail.sysu.edu.cn)

This work was supported in part by the National Natural Science Foundation of China under Grant 61873109.

ABSTRACT This paper proposes an improved intelligent driver model (IDM) by considering the information of multiple front and rear vehicles to describe the car-following behaviour of CAVs (Connected and autonomous vehicles). The model involves the velocity and acceleration of multiple front and rear vehicles as well as the velocity difference and headway between the host vehicle and its surrounding vehicles. By introducing location-related parameters, the model quantitatively expresses the change in influence degree of a surrounding vehicle with its location to the host vehicle. To maximize traffic stability, we obtain the optimal value of the parameters in the model and the effect of specific time delays on the stability of traffic flow with numerical simulation. The results indicate that for a single vehicle control, the proposed model provides a much quicker and smoother acceleration and deceleration process to the desired speed than the IDM and multi-front IDM. And for fleet control, the proposed multi-front and rear IDM is superior to the other two models in decreasing the starting and braking time and increasing the stability of speed and acceleration. With effective car-following behaviour control, it is helpful to improve the operation efficiency of CAVs and enhance the stability of traffic flow. In addition to the car-following behaviour control, the model can be utilized for fleet control in the case of CAVs' homogeneous flow. This model can also serve as an effective tool to simulate car-following behaviour, which is beneficial for road traffic management and infrastructure layout in connected environments.

INDEX TERMS Intelligent driver model (IDM), multi-front and rear vehicle, car-following behavior, traffic flow stability, time delays.

I. INTRODUCTION

Car-following behaviour is a common micro-driving behaviour and describes the interaction between two adjacent vehicles in a single lane with limited overtaking [1]. It has an important impact on traffic flow characteristics, traffic safety and traffic simulation results [2]. The car-following theory is a type of microscopic traffic flow theory, which can accurately describe the complex car-following behaviour and explain the propagation and dissipation mechanism of congestion from the micro level [3]–[5]. It is one of the effective methods to analyse the operation efficiency of the vehicle and stability of traffic flow [6], [7]. Many researchers studied car-following theory to optimize the car-following behaviour, increase the stability of traffic flow and alleviate traffic congestion [8]–[21]. Recent developments of intelligent network technologies enable vehicles to receive information from multiple front and rear vehicles. Thus, the car-following behaviour will be affected by the motion state of the surrounding vehicles. Under this circumstance, it is necessary to study the optimization of the car-following model in connected environments.

Car-following modelling has always been a hot topic in microscopic traffic flow simulation. Traditional car-following models include: the optimal velocity (OV) model [22], generalized force (GF) car-following model [23], and full velocity difference (FVD) model [24]. Most of these models consider the velocity of the host vehicle, velocity difference and headway between the host vehicle and its nearest front vehicle. However, in a connected environment, the connected

The associate editor coordinating the review of this manuscript and approving it for publication was Shajulin Benedict.

and autonomous vehicle (CAV) can obtain accurate motion information from multiple front and rear vehicles. Under this circumstance, some researchers improved the traditional car-following models to adapt to the connected environment. For example, in 2000, Treiber and Helbing *et al.* [25] proposed the intelligent drive model (IDM), which appears to be a good basis for the development of car-following models in a connected environment. This model exhibits controllable stability properties and implements an intelligent braking strategy with smooth transitions between acceleration and deceleration behaviours. However, they did not further investigate whether the IDM could be applied to congested traffic or stop-and-go traffic in urban areas (However, they did not investigate the impact of the vehicles other than the nearest-neighbour ones on the motion state of the host vehicle,), nor did they consider the impact of driving characteristics such as the time delays on the car-following behaviour.

Later, in 2006, Treiber and Kesting *et al.* [25] proposed the human driver (meta-) model (HDM). Compared to the simulation results of the IDM, the HDM reduces the gradients of transitions between free and congested traffic and increases the wavelengths of stop-and-go waves, which is consistent with empirical data. Zhu *et al.* (2006) [27] added a parameter related to the desired time gap in the IDM to solve the problem that the IDM caused a strong breaking manoeuvre when the desired time gap was negative. Moreover, they introduced the time delays so that the model could reflect the complex nonlinear phenomenon of stop-and-go waves. Then, Li *et al.* (2015) [28] and Treiber *et al.* (2006) [29] proposed an extended IDM, which considered the stimulus of multiple front vehicles with linear summation. They substituted the sum of the velocity differences between multiple vehicles ahead and the host vehicle into the IDM to calculate the acceleration of the host vehicle. The results indicated that due to the consideration of the information of multiple front vehicles, the critical value of the stability in the IDM decreased, and the stable region was apparently enlarged.

However, the data show that the effect of the vehicles ahead on the motion of the host vehicle gradually reduces when the distance between them increases, so the front vehicles at different positions have different effects on the host vehicle [30]. How does the distance between the host vehicle and the surrounding vehicles affect the driving behaviour and performance of the overall motorcade? How can one quantitatively express the change in influence degree of a surrounding vehicle with its distance from the host vehicle? The answers to these questions are crucial for controlling the car-following behaviour and improving the traffic flow stability.

Most previous studies on the improved IDM only considered the information of the front vehicles, although in a real world, the vehicles behind also affect the driving decisions of the host vehicle. For example, when the headway between the host vehicle and the rear vehicle is smaller than the desired headway, the host vehicle will accelerate to pursue a safe headway. This situation is especially evident on express ways. To our knowledge, only few studies consider the effect of rear vehicles on the motion of the host vehicle [31]–[33]. Ge *et al.* (2004) [34] proposed an OV model considering a following vehicle. They found that the motion state of the rear vehicle affected the host vehicle. These studies indicate that both front vehicles and rear ones should be involved in car-following control for the host vehicle.

Besides, a few studies proposed that considering cars ahead and following also has effect in stable control of traffic flow. For example, Sun *et al.* (2011) [35] presented an extended car-following model with the consideration of an arbitrary number of cars ahead and one car following on a single-lane highway. The results showed that the combination of backward looking and forward looking effects could further stabilize traffic flow. Monteil *et al.* (2014) [36] studied the stability conditions and shock wave structures of time-continuous car-following models. They indicated that, for strong unstable traffic, the multi-anticipation can remove instabilities. Hence, in a connected environment, it is expected that the traffic flow can be more stable by simultaneously introducing information of both multi-front and rear vehicles into the IDM.

In this paper, we will propose an improved IDM (multi-front and rear IDM) by considering the information of multiple front and rear vehicles. We attempt to quantitatively express the change in influence degree of a surrounding vehicle with its distance from the host vehicle. By involving motion information from multi-front and rear vehicles, the host vehicle's operation efficiency and comfortablemess is expected to increase. In addition to single vehicle control, the multi-front and rear IDM is also expected to achieve a good stability in fleet control. In particular, for a temporary queue (non-pre- planned queue), which consisting of CAVs, it has potential effect in increasing the stability and operation efficiency of the queue and the whole traffic flow.

The organization of this paper is as follows: In Sect. 1, we review the IDM; based on the existing models, the multi-front and rear IDM is constructed in Sect. 2; in Sect. 3, the stability analysis of the proposed model is conducted, and its comparison with the IDM is discussed. The numerical simulation is included in Sect. 4; then, the final section presents the conclusion.

II. MULTI-FRONT AND REAR IDM

When investigating the car-following decision of the host vehicle, most previous studies only considered the information of the front vehicles while neglecting the effect of the rear vehicles. Actually, the information of both front and rear vehicles affects the driving behaviour of the host vehicle [30] . The reason is that the influencing relationship between a preceding and a following vehicle is coupled [30]. When the headway between the host vehicle and the preceding vehicle is smaller than the desired headway, the host vehicle will decelerate to pursue a safe headway. Similarly, the host vehicle tends to accelerate when the headway between it and the rear vehicle approximates to the critical safe value. This is more common for the car-following decision in the

express way scenarios. Studies [21], [33] showed that in addition to the nearest-neighbour vehicles, other front and rear vehicles affect the motion state of the host vehicle, and the influence degree of a surrounding vehicle on the host vehicle gradually reduces when the distance between them increases [34].

Therefore, we propose an improved IDM considering the information of multiple front and rear vehicles (multi-front and rear IDM). The change in influence degree of a front or rear vehicle with its distance from the host vehicle is also quantitatively expressed with the model. The following basic assumptions are made in this paper: (1) There is a succession of vehicles in car following. (2) All vehicles are CAV and form a homogeneous flow.

According to the IDM [25], the acceleration of the host vehicle is composed of two parts. The first part is the acceleration strategy, which can be calculated as:

$$a_n^0[1-(\frac{v_n(t)}{v_n^0})^4] \tag{1}$$

where, a_n^0 and v_n^0 are the maximum acceleration and the desired velocity of n^{th} vehicle in free flow, respectively. $v_n(t)$ is the current velocity of the n^{th} vehicle at time t.

The second part is the braking deceleration strategy, which is defined as follows:

$$-[\tau_f D_f + \boldsymbol{\tau}_r D_r] \tag{2}$$

where, τ_f and τ_r represent the influence weight of front vehicle Q_f and rear vehicle Q_r on the host vehicle, respectively. $\tau_f, \tau_r \epsilon R, 0 \le \tau_f \le 1, 0 \le \tau_r \le 1, \tau_f > \tau_r$ [25] and $0 \le \tau_f + \tau_r \le 1$. D_f and D_r are the sum of the deceleration of multiple front and rear vehicles, respectively. Considering the information of multiple front and rear vehicles (including the desired gap and the maximum acceleration, etc.), we propose the expressions of D_f and D_r by referring to the deceleration term of the IDM:

$$\begin{aligned} D_f = & \sum_{l_f=1}^{Q_f} \xi\left[s^*\left(v_{n-l_f+1}(t), \Delta v_{n-l_f+1}(t)\right)\right] \\ & \times \lambda_{l_f} a^0_{n-l_f+1}\left(\frac{s^*_{n-l_f+1}}{s_{n-l_f+1}}\right) \end{aligned} \tag{3}$$

$$\begin{aligned} D_r = & \sum_{l_r=1}^{Q_r} \xi\left[s^*\left(v_{n+l_r-1}(t), \Delta v_{n+l_r-1}(t)\right)\right] \\ & \times \lambda_{l_r} a^0_{n+l_r-1}\left(\frac{s^*_{n+l_r-1}}{s_{n+l_r-1}}\right) \end{aligned} \tag{4}$$

where, l_f is the l_f^{th} vehicle in front of the host vehicle, l_r is the l_r^{th} vehicle in rear of the host vehicle. $l_f = 1, 2, 3, \ldots, Q_f$ and $l_r = 1, 2, 3, \ldots, Q_r$, in which Q_f and $Q_r (Q_f, Q_r \in \mathrm{N})$ is the number of front and rear vehicles in consideration, respectively. $a^0_{n-l_f+1}$ and $a^0_{n+l_r-1}$ represent the maximum acceleration of the n-l_f+1^{th} vehicle and the $n+l_r$-1^{th} vehicle, respectively.

Peng's [37] study showed that the influence degree of a surrounding vehicle on the host vehicle reduces gradually as the distance between them increases. And Li *et al.* (2010) found that the influence degree is inversely proportional to the distance [30]. In order to express the influence degree of vehicles at different locations on the host vehicle, we introduce the influence weight λ [30] as follows:

$$\begin{aligned} \boldsymbol{\lambda}_{l_f} &= \begin{cases} \dfrac{Q_f - 1}{Q_f^{l_f}}, & for\ l_f \neq Q_f \\ \dfrac{1}{Q_f^{l_f-1}}, & for\ l_f = Q_f, \end{cases} \quad \sum_{l_f=1}^{Q_f} \boldsymbol{\lambda}_{l_f} = 1 \\ \lambda_{l_r} &= \begin{cases} \dfrac{Q_r - 1}{Q_r^{l_r}}, & for\ l_r \neq Q_r \\ \dfrac{1}{Q_r^{l_r-1}}, & for\ l_r = Q_r, \end{cases} \quad \sum_{l_r=1}^{Q_r} \lambda_{l_r} = 1 \end{aligned} \tag{5}$$

where, λ_{l_f} and λ_{l_r} ($\lambda_{l_f}, \lambda_{l_r} \epsilon R$, $\lambda_{l_f}, \lambda_{l_r} \epsilon [0, 1]$) are the influence weight of front and rear vehicles at different locations on the host vehicle, respectively. In the multi-front and rear IDM, λ_{l_f} and λ_{l_r} satisfy the following three conditions:

(1) λ_{l_f} is a monotone decreasing function of l_f, and λ_{l_r} is that of l_r ($l_f > l_{f+1}, l_r > l_{r+1}$).

(2) $\sum_{l_f=1}^{Q_f} \lambda_{l_f} = 1$, $\sum_{l_r=1}^{Q_r} \lambda_{l_r} = 1$

(3) $\lambda_{l_f} = 1$, if $Q_f = 1$ and $Q_r = 0$, and $\lambda_{l_r} = 1$, if $Q_f = 0$ and $Q_r = 1$.

In Eqs. (3) and (4), $s^*_{n-l_f+1}$ and $s^*_{n+l_r-1}$ are the desired gap between each pair of front vehicles and each pair of rear vehicles, respectively. They have equilibrium terms $s_0 + Tv_{n-l_f+1}(t)$ and $s_0 + Tv_{n+l_r-1}(t)$, and dynamic terms $\frac{v_{n-l_f+1}(t)\Delta v_{n-l_f+1}(t)}{2\sqrt{a^0_{v_{n-l_f+1}} b_{n-l_f+1}}}$ and $\frac{v_{n+l_r-1}(t)\Delta v_{n+l_r-1}(t)}{2\sqrt{a^0_{v_{n+l_r-1}} b_{n+l_r-1}}}$. And their expressions are shown in Eq. (6):

$$\begin{aligned} s^*_{n-l_f+1} &= s_0 + Tv_{n-l_f+1}(t) + \frac{v_{n-l_f+1}(t)\Delta v_{n-l_f+1}(t)}{2\sqrt{a^0_{v_{n-l_f+1}} b_{n-l_f+1}}} \\ s^*_{n+l_r-1} &= s_0 + Tv_{n+l_r-1}(t) + \frac{v_{n+l_r-1}(t)\Delta v_{n+l_r-1}(t)}{2\sqrt{a^0_{v_{n+l_r-1}} b_{n+l_r-1}}} \end{aligned} \tag{6}$$

where, s_0 is the minimum space gap for completely stopped traffic. $Tv_{n-l_f+1}(t)$ and $Tv_{n+l_r-1}(t)$ are the velocity-dependent distance, where constant T is the safe time headway. $v_{n-l_f+1}(t)$ and $v_{n+l_r-1}(t)$ are the current velocities of the $n - l_f + 1^{\text{th}}$ vehicle and $n + l_r - 1^{\text{th}}$ vehicle at time t, respectively. $\Delta v_{n-l_f+1}(t) = v_{n-l_f+1}(t) - v_{n-l_f}(t)$ and $\Delta v_{n+l_r-1}(t) = v_{n+l_r}(t) - v_{n+l_r-1}(t)$ are the velocity difference between each pair of front vehicles and each pair of rear vehicles, respectively. b_{n-l_f+1} and b_{n+l_r-1} are the comfortable deceleration of the $n - l_f + 1^{\text{th}}$ vehicle and $n + l_r - 1^{\text{th}}$ vehicle, respectively.

In addition, to solve the problem that the IDM does not conform to the reality when the desired time gap is negative, we introduce two parameters, i.e., $\xi[s^*(v_{n-l_f+1}(t), \Delta v_{n-l_f+1}(t))]$ and $\xi[s^*(v_{n+l_r-1}(t),$

$\Delta v_{n+l_r-1}(t))]$, which are defined as follows:

$$\begin{aligned}
&\xi\left[s^*\left(v_{n-l_f+1}(t), \Delta v_{n-l_f+1}(t)\right)\right] \\
&\quad = \begin{cases} 1, & if\, s^*\left(v_{n-l_f+1}(t), \Delta v_{n-l_f+1}(t)\right) > 0 \\ 0, & if\, s^*\left(v_{n-l_f+1}(t), \Delta v_{n-l_f+1}(t)\right) \le 0 \end{cases} \\
&\xi\left[s^*\left(v_{n+l_r-1}(t), \Delta v_{n+l_r-1}(t)\right)\right] \\
&\quad = \begin{cases} 1, & if\, s^*\left(v_{n+l_r-1}(t), \Delta v_{n+l_r-1}(t)\right) > 0 \\ 0, & if\, s^*\left(v_{n+l_r-1}(t), \Delta v_{n+l_r-1}(t)\right) \le 0 \end{cases}
\end{aligned} \tag{7}$$

According to Eq. (7), we find that when $s^*(v_{n-l_f+1}(t), \Delta v_{n-l_f+1}(t)) \le 0$ or $s^*(v_{n+l_r-1}(t), \Delta v_{n+l_r-1}(t)) \le 0$, for example when a front vehicle moves away from the host vehicle quickly, the host vehicle will adopt the free acceleration strategy, and the deceleration becomes 0.

Accordingly, the acceleration of the host vehicle can be calculated as follows:

$$\begin{aligned}
&a_n(t+t_d) \\
&= a_n^0\left[1-\left(\frac{v_n(t)}{v_n^0}\right)^4\right] - \left[\tau_f D_f + \tau_r D_r\right] \\
&= a_n^0\left[1-\left(\frac{v_n(t)}{v_n^0}\right)^4\right] \\
&\quad -[\tau_f \sum_{l_r=1}^{Q_f} \xi\left[s^*\left(v_{n-l_f+1}(t), \Delta v_{n-l_f+1}(t)\right)\right] \\
&\quad \times \lambda_{l_f} a_{n-l_f+1}^0 \left(\frac{s_{n-l_f+1}^*}{s_{n-l_f+1}}\right)^2 \\
&\quad + \tau_r \sum_{l_r=1}^{Q_r} \xi\left[s^*\left(v_{n+l_r-1}(t), \Delta v_{n+l_r-1}(t)\right)\right] \\
&\quad \times \lambda_{l_r} a_{n+l_r-1}^0 \left(\frac{s_{n+l_r-1}^*}{s_{n+l_r-1}}\right)^2]
\end{aligned} \tag{8}$$

where, $a_n(t+t_d)$ is the acceleration (m/s^2) of the n^{th} vehicle at time $t+t_d$. t_d ($t_d \in$ R) represents the time delays (s).

III. LINEAR STABILITY ANALYSIS AND MODEL CALIBRATION

A. LINEAR STABILITY ANALYSIS

1) STABLE CONDITION ANALYSIS

The stability analysis is crucial for the car-following module [38], [39], which mainly investigates whether the host vehicle can drive free with a safe velocity and distance under the model. In other words, for a larger stability region, collision less likely occurs. We set a basic car-following scenario for the linear stability analysis by giving the following assumptions:

(1) The initial state of the traffic flow is steady, $v_{n+Qr} = \ldots = v_{n+1} = v_n = v_{n-1} \ldots = v_1 = \bar{v}$, where $\bar{v}$ is the average velocity of vehicles.

(2) In the initial state, the length and bumper-to-bumper inter-vehicle clearance is identical for each vehicle, which are defined as l and s, respectively.

The car-following fleet is described as shown in Figure. 1.

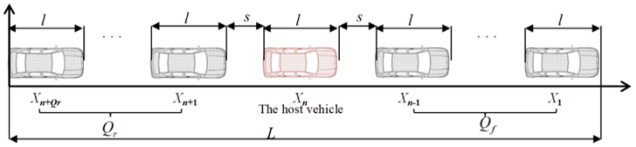

FIGURE 1. Sketch of Car-following Phenomenon.

where, L is the length of the fleet, and X_n is the location of the n^{th} vehicle at time t. Then, we add a disturbance to X_1 in the fleet and analyse the car-following behavior of the following vehicles. Using $f_n(\cdot)$ to express the acceleration under the influence of $s(t)$, $v(t)$ and Δv, we simplify Eq. (8) and get:

$$\begin{aligned}
&\frac{dv_n(t+t_d)}{dt} \\
&= f_n(s(t), v(t), \Delta v) \\
&\quad + \tau_f \sum_{l_f=1}^{Q_f} \lambda_{l_f} f_{n-l_f+1}\left(s_{n-l_f+1}(t), v_{n-l_f+1}(t), \Delta v_{n-l_f+1}\right) \\
&\quad + \tau_r \sum_{l_r=1}^{Q_r} \lambda_{l_r} f_{n+l_r-1}\left(s_{n+l_r-1}(t), v_{n+l_r-1}(t), \Delta v_{n+l_r-1}\right)
\end{aligned} \tag{9}$$

where, $f_n(\cdot)$ represents the acceleration function of the n^{th} vehicle, $f_{n-l_f+1}(\cdot)$ for $n-l_f+1^{\text{th}}$ vehicle and $f_{n+l_r-1}(\cdot)$ for $n+l_r-1^{\text{th}}$ vehicle, respectively. In the initial stable state of traffic flow, the position solution to the stability flow is:

$$\bar{x}_n(t) = (n-1)(\bar{s}+l) + \bar{v}t \tag{10}$$

where, $\bar{x}_n(t)$ is the location of vehicle n at time t without disturbance. In the homogeneous flow, $\bar{s}$ represents the average bumper-to-bumper clearance of adjacent vehicles, and $\bar{v}$ is the average velocity of vehicles. Then we add a disturbance $y_n(t)$ to Eq. (10), it will become:

$$y_n(t) = ce^{i\alpha_k n+zt} = x_n(t) - \bar{x}_n(t), y_n(t) \to 0 \tag{11}$$

where, c is a constant, and $\alpha_k = \frac{2\pi k}{N} (k = 0, 1, \ldots, N-1)$.

$$\begin{aligned}
y_n''(t+t_d) &= x_n''(t+t_d) - \bar{x}''(t+t_d) \\
&= x_n''(t+t_d) = \frac{dv_n(t+t_d)}{dt}
\end{aligned} \tag{12}$$

Substituting Eq. (9) into Eq. (12):

$$\begin{aligned}
&y_n''(t+t_d) \\
&= f_n(s(t), v(t), \Delta v) \\
&\quad + \tau_f \sum_{l_f=1}^{Q_f} \lambda_{l_f} f_{n-l_f+1}\left(s_{n-l_f+1}(t), v_{n-l_f+1}(t), \Delta v_{n-l_f+1}\right) \\
&\quad + \tau_r \sum_{l_r=1}^{Q_r} \lambda_{l_r} f_{n+l_r-1}\left(s_{n+l_r-1}(t), v_{n+l_r-1}(t), \Delta v_{n+l_r-1}\right)
\end{aligned} \tag{13}$$

By linearizing Eq. (13), we then obtain the following equation:

$$\begin{aligned}
&y_n''(t+t_d)\\
&= f_n(y_{n-1}(t)-y_n(t))+f_n^v y_n'(t)+f_n^{\Delta v} y_n'(t)\\
&\quad +f_n^{\Delta v}(y_n'(t)-y_{n-1}'(t))\\
&\quad +\tau_f\sum_{l_f=1}^{Q_f}\lambda_{l_f}\left[f_{n-l_f}^s\left(y_{n-l_f+1}(t)-y_{n-l_f}(t)\right)\right.\\
&\quad \left.+f_{n-l_f}^v y_{n-l_f}'(t)+f_{n-l_f}^{\Delta v}\left(y_{n-l_f}'(t)-y_{n-l_f+1}'(t)\right)\right]\\
&\quad +\tau_r\sum_{l_r=1}^{Q_r}\lambda_{l_r}[f_{n+l_r}^s\left(y_{n+l_f-1}(t)-y_{n+l_r}(t)\right)\\
&\quad +f_{n+l_r}^v y_{n+l_r}'(t)+f_{n+l_r}^{\Delta v}\left(y_{n+l_r}'(t)-y_{n+l_r-1}'(t)\right)]
\end{aligned}\tag{14}$$

where, $f_n^s=\frac{\partial f_n}{\partial s}|_{\bar v,\bar s}\geq 0, f_n^v=\frac{\partial f_n}{\partial v}|_{\bar v,\bar s}\leq 0$ and $f_n^{\Delta v}=\frac{\partial f_n}{\partial \Delta v}|_{\bar v,\bar s}\leq 0$.

We then rewrite Eq. (14) as follows:

$$\begin{aligned}
&y_n'(t+2t_d)-y_n'(t+t_d)\\
&= t_d[f_n^s(y_{n-1}(t)-y_n(t))\\
&\quad +\tau_f\sum_{l_f=1}^{Q_f}\lambda_{l_f}[f_{n-l_f}^s\left(y_{n-l_f-1}(t)-y_{n-l_f}(t)\right)\\
&\quad +\tau_r\sum_{l_r=1}^{Q_r}\lambda_{l_r}f_{n+l_r}^s\left(y_{n+l_f-1}(t)-y_{n+l_r}(t)\right)]\\
&\quad +[f_n^v(y_n(t+t_d)-y_n(t))+\tau_f\sum_{l_f=1}^{Q_f}\lambda_{l_f}f_{n-l_f}^s\\
&\quad \times\left(y_{n-l_f}(t+t_d)-y_{n-l_f}(t)\right)\\
&\quad +\tau_r\sum_{l_r=1}^{Q_r}\lambda_{l_r}f_{n+l_r}^s\left(y_{n+l_r}(t+t_d)-y_{n+l_r}(t)\right)]\\
&\quad +[f_n^{\Delta v}(y_n(t+t_d)-y_n(t))-y_{n-1}(t+t_d)+y_n(t)\\
&\quad +\tau_f\sum_{l_f=1}^{Q_f}\lambda_{l_f}f_{n-l_f}^{\Delta v}\left(y_{n-l_f}(t+t_d)\right.\\
&\quad \left.-y_{n-l_f}(t)-y_{n-l_f-1}(t+t_d)+y_{n-l_f-1}(t)\right)\\
&\quad +\tau_r\sum_{l_r=1}^{Q_r}\lambda_{l_r}f_{n+l_r}^{\Delta v}\left(y_{n+l_r}(t+t_d)\right.\\
&\quad \left.-y_{n+l_r}(t)-y_{n+l_r-1}(t+t_d)+y_{n+l_r-1}(t)\right)]]
\end{aligned}\tag{15}$$

By substituting $y_n(t)=ce^{i\alpha_k n+zt}$ and $y_n'(t)=zce^{i\alpha_k n+zt}$ into Eq. (15) and simplifying the resulting equation, we get:

$$\begin{aligned}
&\left(e^{zt_d}-1\right)[e^{zt_d}-f_n^{\Delta v}\left(1-e^{-i\alpha_k}\right)\\
&\quad -\tau_f\sum_{l_f=1}^{Q_f}\lambda_{l_f}f_{n-l_f}^{\Delta v}\left(e^{-i\alpha_k}-e^{-2i\alpha_k}\right)\\
&\quad -\tau_r\sum_{l_r=1}^{Q_r}\lambda_{l_r}f_{n+l_r}^{\Delta v}\left(e^{-i\alpha_k}-e^{-2i\alpha_k}\right)-f_n^v\\
&\quad -\tau_f\sum_{l_f=1}^{Q_f}\lambda_{l_f}f_{n-l_f}^v e^{-i\alpha_k}-\tau_r\sum_{l_r=1}^{Q_r}\lambda_{l_r}f_{n+l_r}^v e^{i\alpha_k}]\\
&= t_d[f_n^s\left(e^{-i\alpha_k}-1\right)+\tau_f\sum_{l_f=1}^{Q_f}\lambda_{l_f}f_{n-l_f}^s\left(e^{-2i\alpha_k}-e^{-i\alpha_k}\right)\\
&\quad +\tau_r\sum_{l_r=1}^{Q_r}\lambda_{l_r}f_{n+l_r}^s\left(1-e^{i\alpha_k}\right)]
\end{aligned}\tag{16}$$

Expanding $z=z_1(i\alpha_k)+z_2(i\alpha_k)^2+\ldots$ and $e^{zt_d}=1+t_dz+\frac{t_d^2z^2}{2}+\ldots$, and inserting them into Eq. (16), we obtain the first and second-order terms of coefficients in the expression of z respectively, which are given by:

$$z_1=\frac{f_n^s+\tau_f\sum_{l_f=1}^{Q_f}\lambda_{l_f}f_{n-l_f}^s+\tau_r\sum_{l_r=1}^{Q_r}\lambda_{l_r}f_{n+l_r}^s}{f_n^v+\tau_f\sum_{l_f=1}^{Q_f}\lambda_{l_f}f_{n-l_f}^v+\tau_r\sum_{l_r=1}^{Q_r}\lambda_{l_r}f_{n+l_r}^v}\tag{17}$$

$$\begin{aligned}
z_2=&\frac{z_1^2\left(1-\frac{t_d}{2}\left(f_n^v+\tau_f\sum_{l_f=1}^{Q_f}\lambda_{l_f}f_{n-l_f}^v+\tau_r\sum_{l_r=1}^{Q_r}\lambda_{l_r}f_{n+l_r}^v\right)\right)}{f_n^v+\tau_f\sum_{l_f=1}^{Q_f}\lambda_{l_f}f_{n-l_f}^v+\tau_r\sum_{l_r=1}^{Q_r}\lambda_{l_r}f_{n+l_r}^v}\\
&-\frac{\left(\frac{1}{2}f_n^s+\frac{3}{2}\left(\tau_f\sum_{l_f=1}^{Q_f}\lambda_{l_f}f_{n-l_f}^s+\tau_r\sum_{l_r=1}^{Q_r}\lambda_{l_r}f_{n+l_r}^s\right)\right)}{f_n^v+\tau_f\sum_{l_f=1}^{Q_f}\lambda_{l_f}f_{n-l_f}^v+\tau_r\sum_{l_r=1}^{Q_r}\lambda_{l_r}f_{n+l_r}^v}\\
&-\frac{z_1\left(\tau_f\sum_{l_f=1}^{Q_f}\lambda_{l_f}f_{n-l_f}^v+\tau_r\sum_{l_r=1}^{Q_r}\lambda_{l_r}f_{n+l_r}^v+f_n^{\Delta v}\right)}{f_n^v+\tau_f\sum_{l_f=1}^{Q_f}\lambda_{l_f}f_{n-l_f}^v+\tau_r\sum_{l_r=1}^{Q_r}\lambda_{l_r}f_{n+l_r}^v}\\
&-\frac{z_1\left(\tau_f\sum_{l_f=1}^{Q_f}\lambda_{l_f}f_{n-l_f}^{\Delta v}+\tau_r\sum_{l_r=1}^{Q_r}\lambda_{l_r}f_{n+l_r}^{\Delta v}\right)}{f_n^v+\tau_f\sum_{l_f=1}^{Q_f}\lambda_{l_f}f_{n-l_f}^v+\tau_r\sum_{l_r=1}^{Q_r}\lambda_{l_r}f_{n+l_r}^v}
\end{aligned}\tag{18}$$

Since we suppose that in the initial state, all vehicles run with identical clearance s and identical velocity v, $f_n^s=f_{n-l_f}^s=f_{n+l_r}^s, f_n^v=f_{n-l_f}^v=f_{n+l_r}^v$, and $f_n^{\Delta v}=f_{n-l_f}^{\Delta v}=f_{n+l_r}^{\Delta v}$ are satisfied.

When $z_2>0$, we get:

$$\frac{t_d}{2}<\frac{1}{f_n^v(1+\tau_f+\tau_r)}-\frac{f_n^{\Delta v}+f_n^v\left[\frac{1}{2}+\frac{5}{2}(\tau_f+\tau_r)\right]}{f_n^s}\tag{19}$$

According to Eqs. (6) and (9), we obtain the specific form of f_n^s, f_n^v and $f_n^{\Delta v}$ as follows:

$$\begin{aligned}
f_n^s=&\frac{2}{s_{lf}}\tau_f\sum_{l_{f=1}}^{Q_f}\lambda_{l_f}a_{n-l_f+1}^0\left(\frac{s_0+Tv_{n(t)}}{s_{n-l_f+1}(t)}\right)^2\\
&+\frac{2}{s_{l_r}}\tau_r\sum_{l_{r=1}}^{Q_r}\lambda_{l_r}a_{n+l_r-1}^0\left(\frac{s_0+Tv_{n(t)}}{s_{n+l_r-1}(t)}\right)^2\\
f_n^v=&-2\left(a_n^0\frac{2}{v_n^0}\left(\frac{v_n}{v_n^0}\right)^3+\tau_f\sum_{l_{f=1}}^{Q_f}\lambda_{l_f}a_{n-l_f+1}^0\right.
\end{aligned}\tag{20}$$

$$\times \left(\frac{T\left(s_0 + Tv_n(t)\right)}{s^2_{n-l_f+1}(t)} \right) + \tau_r \sum_{l_r=1}^{Q_r} \lambda_{l_r} a^0_{n+l_r-1} \left(\frac{T\left(s_0 + Tv_n(t)\right)}{s^2_{n+l_f-1}(t)} \right) \Bigg) \quad (21)$$

$$f_n^{\Delta v} = \tau_f \sum_{l_f=1}^{Q_f} \lambda_{l_f} \frac{v_n(t)(s_0+Tv_n(t))}{s_{n-l_f+1}(t)} \sqrt{\frac{a^0_{n-l_f+1}}{b_{n-l_f+1}}} + \tau_r \sum_{l_r=1}^{Q_r} \lambda_{l_r} \frac{v_n(t)(s_0+Tv_n(t))}{s_{n-l_r+1}(t)} \sqrt{\frac{a^0_{n+l_r-1}}{b_{n+l_r-1}}} \quad (22)$$

By substituting Eq. (20)-(22) into Eq. (19), the stability condition can be expressed as (23), shown at the bottom of the page.

According to Eq. (19), the linear stability assays were carried out as follows:

(1) When $t_d = \tau_f = \tau_r = 0$, the result of stable conditions in the multi-front and rear IDM is the same as that of the IDM [40]:

$$f_n^v f_n^{\Delta v} + \frac{1}{2}(f_n^v)^2 - f_n^s > 0 \quad (24)$$

(2) When $t_d = 0$, $\tau_f \neq 0$ and $\tau_r \neq 0$, the result of stable conditions in the multi-front and rear IDM is:

$$f_n^v f_n^{\Delta v}(1+\tau_f+\tau_r) + \frac{1}{2}\left(\frac{5}{2}(\tau_f+\tau_r)\right)(f_n^v)^2 - f_n^s > 0 \quad (25)$$

where, τ_f and τ_r are not negative and $0 \leq \tau_f + \tau_r < 1$.

Comparing the result with that of the IDM, we find:

$$f_n^v f_n^{\Delta v}\left(1 + \tau_f + \tau_r\right) + \frac{1}{2}\left(\frac{5}{2}\left(\tau_f + \tau_r\right)\right)\left(f_n^v\right)^2 - f_n^s > f_n^v f_n^{\Delta v} + \frac{1}{2}(f_n^v)^2 - f_n^s \quad (26)$$

In other words, by introducing the information of multiple front and rear vehicles, the traffic flow becomes more stable than that with the IDM. The results also show that when more front and rear vehicles are considered, the traffic is more stable.

2) STABLE CURVES ANALYSIS

Successively, we will depict the critical stable curves for different models and analyse the influence degree of the front and rear vehicles on the host vehicle and the effect of the number of front and rear vehicles on the stability of the traffic flow under the model. Figure. 2 shows the critical stable curves for six sets of eigenvalues when the time delays is equal to 0, i.e., the critical stable curves of the IDM ($\tau_f = 0$, $\tau_r = 0$, $Q_f = 1$, $Q_r = 0$), multi-front IDM ($\tau_f = 0.1$, $\tau_r = 0$, $Q_f = 2$, $Q_r = 0$), multi-front IDM ($\tau_f = 0.1$, $\tau_r = 0$, $Q_f = 5$, $Q_r = 0$), multi-front and rear IDM ($\tau_f = 0.1$, $\tau_r = 0$, $Q_f = 5$, $Q_r = 1$), multi-front and rear IDM ($\tau_f = 0.1$, $\tau_r = 0.1$, $Q_f = 5$, $Q_r = 2$), and multi-front and rear IDM ($\tau_f = 0.2$, $\tau_r = 0.2$, $Q_f = 5$, $Q_r = 2$). The critical stable curve presents the jamming transition curve of the free traffic, inhomogeneous coexisting phase, and homogeneous congested traffic. The regions above and under the critical stability curve are called the stable region and unstable region, respectively. A point in the stable region indicates that the traffic flow is stable and there is no congestion, while a point in the unstable region indicates an unstable traffic flow and density waves.

The results show that the stable regions of multi-front IDM ($\tau_f = 0.1$, $\tau_r = 0$, $Q_f = 2$, $Q_r = 0$) and multi-front IDM ($\tau_f = 0.1$, $\tau_r = 0$, $Q_f = 5$, $Q_r = 0$) are larger than that of the IDM ($\tau_f = 0$, $\tau_r = 0$, $Q_f = 1$, $Q_r = 0$). Thus, the stability of traffic flow under the multi-front IDM is better than that under the IDM. The stable region of the multi-front IDM with five front vehicles ($\tau_f = 0.1$, $\tau_r = 0$, $Q_f = 5$, $Q_r = 0$) is larger than that with involving two preceding vehicles ($\tau_f = 0.1$, $\tau_r = 0$, $Q_f = 2$, $Q_r = 0$). Thus, the stability of traffic flow under the multi-front IDM with five front vehicles is better than that with two front vehicles. In addition to five front vehicles, we consider one rear vehicle (multi-front and

$$\frac{t_d}{2} < \frac{1}{-2\left(1+\tau_f+\tau_r\right)} \frac{1}{-2\left(a_n^0 \frac{2}{v_n^0}\left(\frac{v_n}{v_n^0}\right)^3 + \tau_f \sum_{l_f=1}^{Q_f} \lambda_{l_f} a^0_{n-l_f+1}\left(\frac{T(s_0+Tv_n(t))}{s^2_{n-l_f+1}(t)}\right) + \tau_r \sum_{l_r=1}^{Q_r} \lambda_{l_r} a^0_{n+l_r-1}\left(\frac{T(s_0+Tv_n(t))}{s^2_{n-l_f-1}(t)}\right)\right)\left(1+\tau_f+\tau_r\right)} - \frac{\tau_f \sum_{l_f=1}^{Q_f} \lambda_{l_f} \frac{v_{n(t)}(s_0+Tv_{n(t)})}{s_{n-l_f+1}(t)} \sqrt{\frac{a^0_{n-l_f+1}}{b_{n-l_f+1}}} + \tau_r \sum_{l_r=1}^{Q_r} \lambda_{l_r} \frac{v_{n(t)}(s_0+Tv_{n(t)})}{s_{n-l_r+1}(t)} \sqrt{\frac{a^0_{n-l_r+1}}{b_{n-l_r+1}}}}{\left[\frac{2}{s_{l_f}} \tau_f \sum_{l_f=1}^{Q_f} \lambda_{l_f} a^0_{n-l_f+1}\left(\frac{s_0+Tv_{n(t)}}{s_{n-l_f+1}(t)}\right)^2 + \frac{2}{s_{l_r}} \tau_r \sum_{l_r=1}^{Q_r} \lambda_{l_r} a^0_{n+l_r-1}\left(\frac{s_0+Tv_{n(t)}}{s_{n+l_f-1}(t)}\right)^2\right]\left(1+\tau_f+\tau_r\right)} - \frac{\left[\frac{1}{2}+\frac{5}{2}\left(\tau_f+\tau_r\right)\right]\left[-2\left(a_n^0 \frac{2}{v_n^0}\left(\frac{v_n}{v_n^0}\right)^3 + \tau_f \sum_{l_f=1}^{Q_f} \lambda_{l_f} a^0_{n-l_f+1} \frac{T\left(s_0+Tv_{n(t)}\right)}{s^2_{n-l_f+1}(t)} + \tau_r \sum_{l_r=1}^{Q_r} \lambda_{l_r} a^0_{n+l_r-1} \frac{T\left(s_0+Tv_{n(t)}\right)}{s^2_{n+l_f-1}(t)}\right)\right]}{\left[\frac{2}{s_{l_f}} \tau_f \sum_{l_f=1}^{Q_f} \lambda_{l_f} a^0_{n-l_f+1}\left(\frac{s_0+Tv_{n(t)}}{s_{n-l_f+1}(t)}\right)^2 + \frac{2}{s_{l_r}} \tau_r \sum_{l_r=1}^{Q_r} \lambda_{l_r} a^0_{n+l_r-1}\left(\frac{s_0+Tv_{n(t)}}{s_{n+l_f-1}(t)}\right)^2\right]\left(1+\tau_f+\tau_r\right)} \quad (23)$$

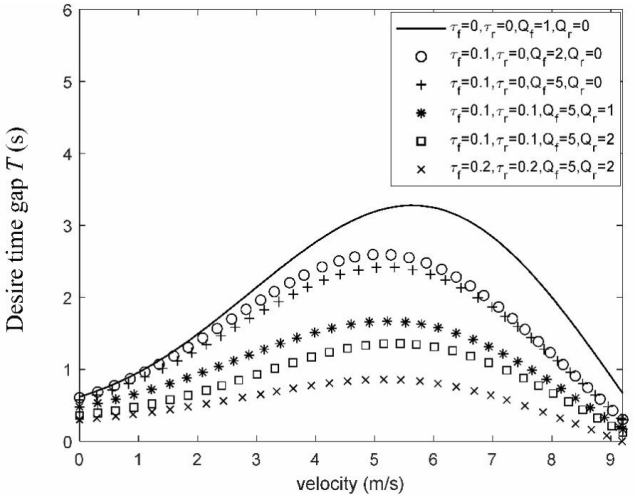

FIGURE 2. The Critical Stable Curves Corresponding to Six Sets of Eigenvalues ($t_d = 0$).

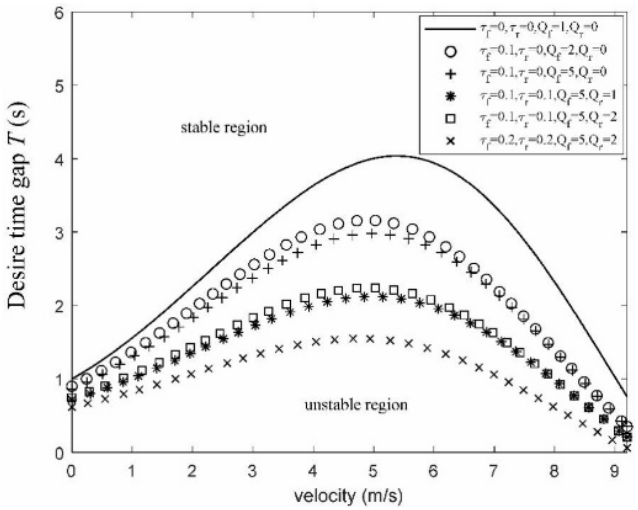

FIGURE 3. The Critical Stable Curves Corresponding to Six Sets of Eigenvalues ($t_d = 1$s).

rear IDM, $\tau_f = 0.1$, $\tau_r = 0.1$, $Q_f = 5$, $Q_r = 1$) and two rear vehicles (multi-front and rear IDM, $\tau_f = 0.1$, $\tau_r = 0.1$, $Q_f = 5$, $Q_r = 2$). We find that the stable region of the multi-front and rear IDM ($\tau_f = 0.1$, $\tau_r = 0.1$, $Q_f = 5$, $Q_r = 1$) is larger than those of the multi-front IDM and IDM. In other words, the stability of traffic flow under the multi-front and rear IDM is better than that with no rear vehicle. Moreover, the multi-front and rear IDM with two rear vehicles obtains a larger stable region than that with one following vehicle.

The results show that the multi-front and rear IDM has better stability of traffic flow than the multi-front IDM and IDM because the host vehicle receives more information with more front and rear vehicles. Then, the driver obtains the operation trend of the entire fleet and make a relatively more effective car-following decision in advance to achieve the effect of a smooth operation, which will effectively reduce the intensity of the disturbance on the surrounding vehicles to the host vehicle, speed up the dissipation of the disturbance, and improve the stability of traffic flow.

Moreover, Figure. 3 depicts the critical state curves of the six situations with time delays $t_d = 1$ s. The results are similar to that when $t_d = 0$, which shows a more stable condition from the multi-front and rear IDM than those from the IDM and multi-front IDM, regardless of whether there is delay. Additionally, when the number of front and rear vehicles and the sensitivity coefficients increase, the stable regions of the model are gradually expanded. To quantitatively compare the differences among these models, we integrate the unstable region of each model in two cases ($t_d = 0$ s and $t_d = 1$ s) and calculate the corresponding increasing rate of the area of the stable region.

As shown in Table 1, compared with the unstable region of each model when $t_d = 0$ s, the instability of the corresponding model when $t_d = 1$ s increases, probably since the increase in reaction time delays the car-following decision and adjusts the movement state of vehicles. Within the time delays, the surrounding condition of the host vehicle has changed, so the successive car-following decisions may no longer be optimal. Furthermore, when the considered number of front and rear vehicles increases, the effect of the time delays on the traffic flow stability will gradually accumulate. Thus, the possibility of traffic congestion increases. However, because the car-following behaviour with time delays is more consistent with the actual situation, in the following analysis, we will consider the effect of the time delays on the stability of traffic flow.

TABLE 1. Area of unstable region.

Model	unstable region ($t_d = 0$ s)	unstable region ($t_d = 1$ s)	Increasing rate (%)
IDM $\tau_f = 0$, $\tau_r = 0$, $Q_f = 1$, $Q_r = 0$	19.85	25.61	29.07
multi-front IDM $\tau_f = 0.1$, $\tau_r = 0$, $Q_f = 2$, $Q_r = 0$	15.55	19.56	25.79
multi-front IDM $\tau_f = 0.1$, $\tau_r = 0$, $Q_f = 5$, $Q_r = 0$	14.59	18.60	27.48
multi-front and rear IDM $\tau_f = 0.1$, $\tau_r = 0.1$, $Q_f = 5$, $Q_r = 1$	10.22	13.43	31.41
multi-front and rear IDM $\tau_f = 0.1$, $\tau_r = 0.1$, $Q_f = 5$, $Q_r = 2$	8.07	11.17	38.41
multi-front and rear IDM $\tau_f = 0.2$, $\tau_r = 0.2$, $Q_f = 5$, $Q_r = 2$	5.18	7.29	40.73

B. MODEL CALIBRATION

Theoretically, the stability of traffic flow gradually increases when Q_f, Q_r, τ_f and τ_r increase. However, in real-world traffic, it is not necessary to consider the information from all front and rear vehicles. With the increase in distance from a surrounding vehicle to the host vehicle, the impact gradually decreases until it becomes approximately zero when the distance is sufficiently large. In addition, the excessive information will increase the time required for the driver to perceive, process and make a decision. Therefore, it is necessary to determine the proper number for the influential front vs. rear vehicles and the corresponding sensitive coefficients in the multi-front and rear IDM.

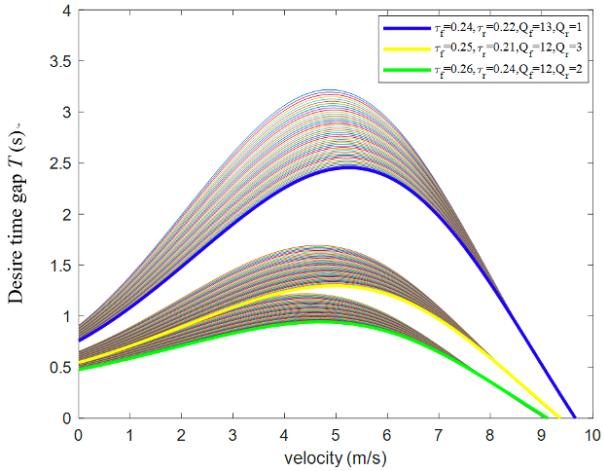

FIGURE 4. The Critical Stable Curves (t_d = 1s).

In this paper, we will use numerical simulation to optimize the parameters in the multi-front and rear IDM with $t_d = 1$ s. According to previous studies [37], the ranges of τ_f and τ_r are set to 0-0.3 with a step length of 0.01, and the ranges of Q_f and Q_r are 0-3 with a step length of 1. To maximize the car-following stability, we traverse all values in the above range to find the corresponding optimal value in the multi-front and rear IDM. The results in Figure. 4 indicate that there are three clusters of critical stable curves. Cluster I, Cluster II and Cluster III represent the critical stable curves with $Q_r = 1$, $Q_r = 2$ and $Q_r = 3$, respectively.

For convenience of comparison, in each cluster, we find the lowest critical stable curves, which are $\tau_f = 0.24, \tau_r = 0.22$, $Q_f = 13$, $Q_r = 1$ (the blue line in Figure. 4), $\tau_f = 0.25, \tau_r = 0.21, Q_f = 12$, $Q_r = 3$ (yellow line), and, $\tau_f = 0.26, \tau_r = 0.24, Q_f = 12$, $Q_r = 2$ (green line). The results show that when $\tau_f = 0.26, \tau_r = 0.24$, $Q_f = 12$ and $Q_r = 2$, the multi-front and rear IDM has the best stability of traffic flow among these three curves, which indicates the optimal value of the corresponding parameters in the model. By substituting the calibration results into Eq. (8), we obtain the acceleration equation of the multi-front and rear IDM with $t_d = 1$ s:

$$\begin{aligned} & a_n(t+t_d) \\ & = a_n^0\left[1-\left(\frac{v_n(t)}{v_n^0}\right)^4\right] \\ & \quad -[0.26\sum_{l_f=1}^{Q_f=12}\xi\left[s^*\left(v_{n-l_f+1}(t),\Delta v_{n-l_f+1}(t)\right)\right] \\ & \quad \times\lambda_{l_f}a_{n-l_f+1}^0\left(\frac{s_{n-l_f+1}^*}{s_{n-l_f+1}}\right)^2 \\ & \quad +0.24\sum_{l_r=1}^{Q_r=2}\xi\left[s^*\left(v_{n+l_r-1}(t),\Delta v_{n+l_r-1}(t)\right)\right]\lambda_{l_r}a_{n+l_r-1}^0 \\ & \quad \times\left(\frac{s_{n+l_r-1}^*}{s_{n+l_r-1}}\right)^2] \end{aligned} \tag{27}$$

IV. NUMERICAL SIMULATION AND RESULT ANALYSIS

To analyse the dynamic performance of the multi-front and rear IDM, a numerical simulation is performed. We assume that there are 100 vehicles running in a single lane with the total length as $L = 2000$ m. The initial conditions are set as follows: $a_n^0 = a_{n+1}^0 + a_{n+2}^0 = 1$ m/s; $s_0 = 2$ m; $t_d = 1$ s; $v_0 = 20$ m/s; $T = 1$ s; $b = 1.5$ s; $l = 5$ m; $s = 15$ m. In the initial state, the fleet remains static. For model validation, we set up two typical scenes: starting acceleration process and braking deceleration process:

(1) Starting process: When $t = 0$ s, the first vehicle starts and speeds up until it reaches and maintains a constant speed of 20 m/s. The initial steady state will be broken when the other vehicles begin to follow it.

(2) Deceleration process: When $t = 400$ s, the first vehicle brakes and decreases from 20 m/s to 10 m/s, and the following vehicles decelerate until each following vehicle reaches the speed of 10 m/s.

We use the fourth-order Runge-Kutta algorithm for numerical integration with the time-step $\Delta t = 0.01$ s. For convenience of comparison, identical initial conditions in the IDM and multi-front IDM are set to those in the multi-front and rear IDM.

A. VELOCITY CHANGING ANALYSIS

The changes in velocity of all vehicles in the IDM, multi-front IDM, and multi-front and rear IDM are shown in Figure 5. The results indicate that in the starting process, the velocity of each vehicle under the IDM sequentially increases from 0, and all vehicles finish the starting process at $t = 125$ s. The reason is that the following vehicles decide to accelerate or decelerate only based on the motion state of the nearest front vehicle. The vehicle controlled by the multi-front IDM involves the acceleration information of multiple front

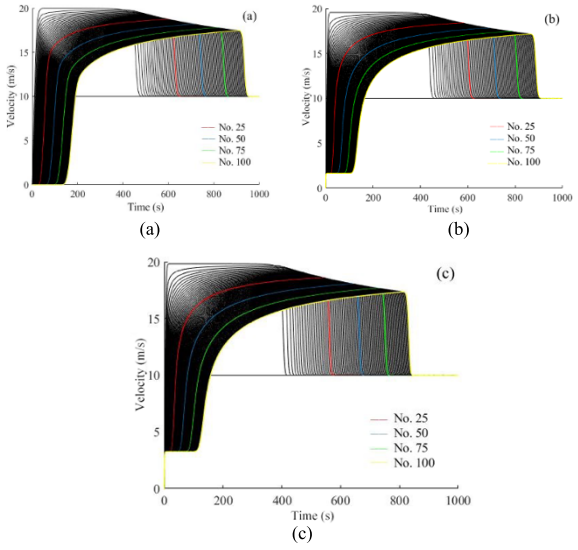

FIGURE 5. The Velocity Distribution of Vehicles (a) IDM (b) multi-front IDM (c) multi-front and rear IDM.

vehicles in its car-following decision. After the first vehicle begins speeding up, the following vehicles begin their decision-making process. The results show that their velocities gradually increase under the multi-front IDM, and all vehicles complete the starting process at $t = 114$ s. If we take the queue of 100 vehicles in this case as a fleet, the starting process of the whole fleet the multi-front IDM is faster than that of the IDM, which reveals a good performance in fleet control. Furthermore, under the multi-front and rear IDM, each vehicle receives the acceleration information of multiple vehicles ahead and rear vehicles. Therefore, its starting process is faster than both IDM and multi-front IDM. The results indicate that the time of the starting process reduces by 19.2% and 11.4% compared to those of the IDM and multi-front IDM, respectively.

As for the deceleration process of the fleet, the results indicate that it takes less time for the vehicles in the fleet to decelerate to 10 m/s under the multi-front and rear IDM than under the IDM and multi-front IDM. Compared to the latter two, the deceleration efficiency under the multi-front and rear IDM is improved by 17.8% and 10.7%, respectively. The reason is that the vehicles under the multi-front and rear IDM obtain the deceleration information of multiple front vehicles during the entire simulation. Based on this information, the driver decides to decelerate in advance to achieve the effect of a smooth operation. In addition, the deceleration information of multiple rear vehicles can improve the deceleration stability of the host vehicle and reduce unnecessary disturbance and collision probability.

To make a more detailed comparison of the velocity changes among the three models in a single vehicle control, we analyze the distributions of the acceleration and deceleration of the 25th, 50th, 75th and 100th vehicle as shown in Table 2, where a_{max}^{acc} is the maximum acceleration in the starting process, a_{max}^{dec} is the maximum deceleration in the braking process, and a_{ave}^{acc} and a_{ave}^{dec} are the average acceleration and average deceleration, respectively.

The results indicate that, when a vehicle approaches the upstream position, its a_{max}^{acc}, a_{max}^{dec}, a_{ave}^{acc} and a_{ave}^{dec} decrease in both models. The reason is possibly that the velocity perturbation generated by the downstream vehicles gradually weakens in the process of propagating upstream. For example, when the distance from the perturbation propagation increases, the average acceleration of the 75th vehicle, which is upstream, is lower than that of the 25th vehicle downstream. For the comparison of different models, the average maximum acceleration in the overall starting process under the multi-front and rear IDM is 31.11% lower than that under the IDM. Similarly, we obtain a 26.22% reduction of the average maximum deceleration for the braking process. In actual traffic conditions, the decrease in peak acceleration will avoid generating a large perturbation caused by the excessive velocity change and effectively suppress the generation of stop-and-go waves to reduce the possibility of congestion and rear-end collision. Additionally, the driver can obtain more sufficient time to handle suddenly occurring traffic by receiving the movement information of multiple front and rear vehicles in time. This information helps them make car-following decisions earlier, which will lead to a smooth transition between different driving states and increase the traffic stability.

TABLE 2. The Acceleration and Deceleration of 25th, 50th, 75th and 100th vehicles.

No.	Parameter	Model	Value (m/s^2)
25	a_{max}^{acc}	IDM	2.54
		multi-front IDM	1.94
		multi-front and rear IDM	1.81
	a_{max}^{dec}	IDM	-1.86
		multi-front IDM	-1.51
		multi-front and rear IDM	-1.42
	a_{ave}^{acc}	IDM	1.37
		multi-front IDM	1.02
		multi-front and rear IDM	0.96
	a_{ave}^{dec}	IDM	-1.53
		multi-front IDM	-1.07
		multi-front and rear IDM	-0.91
50	a_{max}^{acc}	IDM	2.31
		multi-front IDM	1.68
		multi-front and rear IDM	1.56
	a_{max}^{dec}	IDM	-1.74
		multi-front IDM	-1.34
		multi-front and rear IDM	-1.23
	a_{ave}^{acc}	IDM	1.24
		multi-front IDM	0.91
		multi-front and rear IDM	0.88
	a_{ave}^{dec}	IDM	-1.46
		multi-front IDM	-0.96
		multi-front and rear IDM	-0.82
75	a_{max}^{acc}	IDM	-1.58
		multi-front IDM	-1.2
		multi-front and rear IDM	-1.17
	a_{max}^{dec}	IDM	1.13
		multi-front IDM	0.83
		multi-front and rear IDM	0.78
	a_{ave}^{acc}	IDM	-1.39
		multi-front IDM	-0.85
		multi-front and rear IDM	-0.74
	a_{ave}^{dec}	IDM	1.92
		multi-front IDM	1.4
		multi-front and rear IDM	1.33
100	a_{max}^{acc}	IDM	-1.38
		multi-front IDM	-1.06
		multi-front and rear IDM	-1.02
	a_{max}^{dec}	IDM	1.01
		multi-front IDM	0.77
		multi-front and rear IDM	0.66
	a_{ave}^{acc}	IDM	-1.27
		multi-front IDM	-0.73
		multi-front and rear IDM	-0.68
	a_{ave}^{dec}	IDM	-1.58
		multi-front IDM	-1.2
		multi-front and rear IDM	-1.17

B. POSITION CHANGING ANALYSIS

Successively, Figure. 6 shows the position distribution of the three models obtained from the simulation process. In the starting process for the fleet control, all following vehicles under the IDM remain in the initial position because the drivers do not make the car-following decision until the nearest front vehicle begins to accelerate, since they do not use the

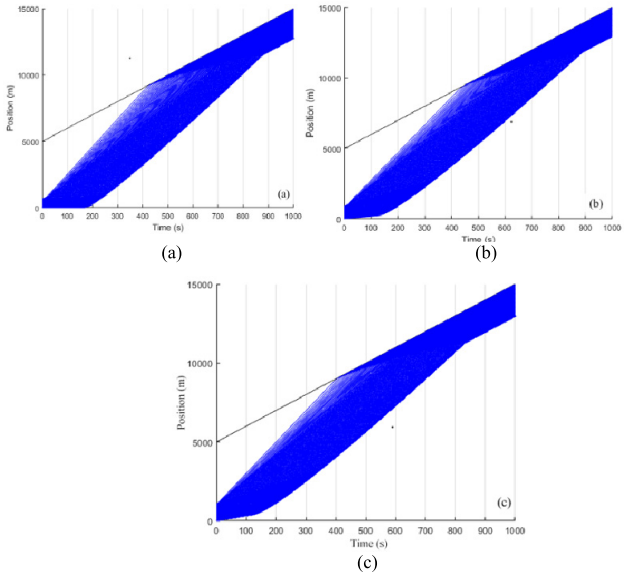

FIGURE 6. The Position Distribution of Vehicles (a) IDM (b) multi-front IDM (c) multi-front and rear IDM.

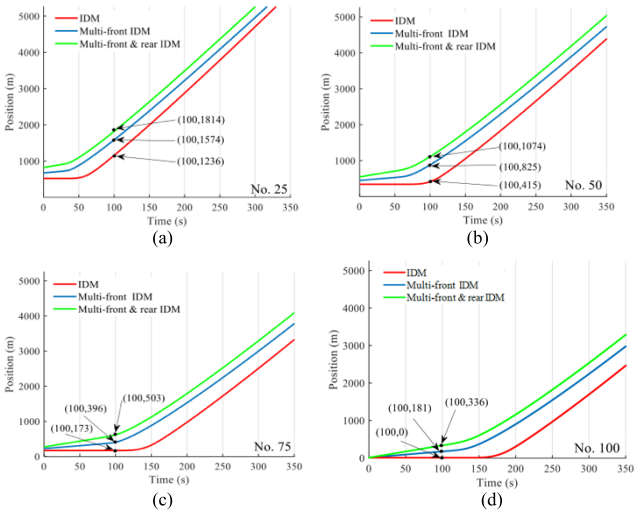

FIGURE 7. The Position Distribution of Vehicles (a) the 25th vehicle (b) the 50th vehicle (c) the 75th vehicle (d) the 100th vehicle.

acceleration information of multiple front and rear vehicle in decision making. By comparison, with the multi-front IDM in the simulation, after the first vehicle starts accelerating and changes its position, all following vehicles successively start accelerating. The positional change of the following vehicles under the multi-front and rear IDM is even faster than that under the multi-front IDM. Specifically, in Figure. 7, we compare the positions of the 25th, 50th, 75th and 100th vehicles at $t = 100$ s. The data indicate that the multi-front and rear IDM has the large position changes among the three models, especially for the 100th vehicle. The results indicate that for a single vehicle control, the position of the 100th vehicle under the IDM does not change at all when $t = 100$ s, while that under the multi-front IDM is 181 m and that under the multi-front and rear IDM is 336 m. Similarly, the position changes of other vehicles are different among the three models. For example, the position of the 25th vehicle at $t = 100$ s in the IDM is 1,236 m and that in the multi-front and rear IDM is 1,814 m, which is 578 m ahead of the 100th vehicle in the IDM. Thus, the following vehicles can accelerate faster in the starting process under the multi-front and rear IDM, which helps them reach a stable state as soon as possible.

In the braking process, the velocity of the first vehicle under the IDM vs. multi-front IDM reaches 10 m/s at $t = 432$ s vs. $t = 414$ s, and the state of the entire fleet becomes stable at $t = 881$ s vs. $t = 873$ s, respectively. By comparison, under the multi-front and rear IDM, the velocity of the first vehicle reaches a speed of 10 m/s at $t = 391$ s, which is 41 s earlier than the multi-front IDM and 50 s earlier than the IDM.

Therefore, based on the movement information of multiple front and rear vehicles, the multi-front and rear IDM can be effectively utilized to control the car-following behaviour of drivers and reduce the effect of disturbance during the car-following process to improve the operation efficiency of the fleet and stability of the traffic flow.

V. CONCLUSION

This paper proposes the multi-front and rear IDM to describe the microscopic car-following behaviour in a connected environment. The model employs the information of multiple front and rear vehicles in calculating the acceleration of the host vehicle. In addition to the parameters of velocity and acceleration, the model considers the velocity difference and headway between the host vehicle and its surrounding vehicles. By adding weights λ_{l_f} and λ_{l_r} for the front and rear vehicles, respectively, the model quantitatively expresses the change of their influence degree on the host vehicle with its distance. Additionally, we introduce $\xi\left[s^*\left(v_{n-l_f+1}(t), \Delta v_{n-l_f+1}(t)\right)\right]$ and $\xi\left[s^*\left(v_{n+l_r-1}(t), \Delta v_{n+l_r-1}(t)\right)\right]$ to solve the problem that the IDM will cause a strong breaking manoeuvre when the desired time gap is negative.

According to the linear stability analysis results, the traffic flow under the multi-front and rear IDM is more stable than those under the IDM and multi-front IDM. The traffic stability gradually increases when the considered number of front and rear vehicles increases. In addition, we investigate the effect of the time delays on the stability of traffic flow. The results indicate that the accumulation of time delays from multiple front and rear vehicles in the car-following fleet increases its instability, which is accordant with actual traffic conditions. Taking 1 s as the time delays and the maximizing car-following stability as the calibration target, we conduct the numerical simulation and obtain the optimal values of the parameters in the model, i.e., $\tau_f = 0.26, \tau_r = 0.24, Q_f = 12$ and $Q_r = 2$.

In single vehicle control, the results of numerical simulation indicate that the average maximum acceleration of the 25th vehicles under the multi-front and rear IDM decreases by 31.11% compared to the IDM and 10.57% compared to the multi-front IDM. Its average maximum deceleration

under the multi-front and rear IDM decreases by 23.7% compared to the IDM and 5.9% compared to the multi-front IDM. Similarly, compared to the IDM and multi-front IDM, the average acceleration of the 50th vehicles under the multi-front and rear IDM decreases by 29.1% and 3.3%, respectively. And the average acceleration of other vehicles under the multi-front and rear IDM are smaller than that in the other two models. Thus, the vehicle controlled by the multi-front and rear IDM can more smoothly accelerate and decelerate to the desired speed than that by the other two models.

The results of numerical simulation indicate that the time for the fleet of 100 vehicles to finish the starting process under the multi-front and rear IDM is reduced by 19.2% compared to the IDM and 11.4% compared to the multi-front IDM. In addition, compared to the IDM and multi-front IDM, the deceleration efficiency under the multi-front and rear IDM improves by 17.8% and 10.7%, respectively. The time to reach a stable state under the multi-front and rear IDM is 42 s less than the IDM and 34 s less than the Multi-front IDM. Therefore, compared with the IDM and multi-front IDM, the car-following behaviour is more stable, and the operation state of a fleet under the multi-front and rear IDM is more stable. This result reveals the benefit of introducing the motion state of multiple front and rear vehicles in car-following behaviour modelling. Controlled by the multi-front and rear IDM, the car-following behaviour becomes gentler. The model also effectively suppresses the propagation of disturbance, speeds up its dispersal, increases the stability of the fleet and reduces the possibility of traffic congestion.

In this paper, in order to accurately obtain the effect of time delays t_d on the stability of traffic flow, we integrate the unstable region of each model in two cases ($t_d = 0$ s and $t_d = 1$ s) to obtain their areas and calculate the corresponding increasing rate of the stable area. The results indicate that the traffic flow when $t_d = 0$ s is the most stable among all t_d values. Compared with the area of the unstable region when $t_d = 0$ s, the unstable area when $t_d = 1$ s increases by 40.73% under the multi-front and rear IDM. Similarly, in the IDM and multi-front IDM, the increase in time delays also increases the instability of traffic flow. This result is consistent with the actual situation, i.e., the increase in time delays leads to a delay in making the car-following decision and adjusting the vehicle motion, which makes the traffic flow gradually unstable and begin to generate density waves. With the development of intelligent network technologies, the time delays will gradually decrease, which is helpful to reduce the disturbance caused by the time delays and improve the stability of traffic flow.

Notably, this paper only addresses the car-following modelling for a homogeneous flow. Further research can focus on simulating a heterogeneous flow in a connected environment. Additionally, the effect of different time delays on the stability of traffic flow must be further discussed.

REFERENCES

[1] M. Brackstone and M. McDonald, "Car-following: A historical review," *Transp. Res. F, Traffic Psychol. Behav.*, vol. 2, no. 4, pp. 181–196, Dec. 1999.

[2] T. Toledo, "Driving behaviour: Model and challenges," *Transp. Rev.*, vol. 27, no. 1, pp. 65–84, 2007.

[3] G. F. Newell, "Memoirs on highway traffic flow theory in the 1950s," *Oper. Res.*, vol. 50, no. 1, pp. 173–178, Feb. 2002.

[4] R. E. Chandler, R. Herman, and E. W. Montroll, "Traffic dynamics: Studies in car following," *Oper. Res.*, vol. 6, no. 2, pp. 165–184, Apr. 1958.

[5] D. C. Gazis, "The origins of traffic theory," *Oper. Res.*, vol. 50, no. 1, pp. 69–77, Feb. 2002.

[6] A. Reuschel, "Vehicle movements in the column uniformly accelerated for delayed," *Oesterrich Ingr. Arch.*, vol. 4, pp. 193–215, Jan. 1950.

[7] L. A. Pipes, "An operational analysis of traffic dynamic," *J. Appl. Phys.*, vol. 24, no. 3, pp. 274–281, 1953.

[8] J. L. David and S. A. Paul, "A nonlinear temporal headway model of traffic dynamics," *Nonlinear Dyn.*, vol. 16, pp. 127–151, Jun. 1998.

[9] S. Ossen and S. P. Hoogendoorn, "Car-following behavior analysis from microscopic trajectory data," *Transp. Res. Record, J. Transp. Res. Board*, vol. 1934, no. 1, pp. 13–21, Jan. 2005.

[10] J. W. Ro, P. S. Roop, A. Malik, and P. Ranjitkar, "A formal approach for modeling and simulation of human car-following behavior," *IEEE Trans. Intell. Transp. Syst.*, vol. 19, no. 2, pp. 639–648, Feb. 2018.

[11] J. Kim and H. S. Mahmassani, "Correlated parameters in driving behavior models: Car-following example and implications for traffic microsimulation," *Transp. Res. Rec., J. Transp. Res. Board*, vol. 2249, no. 1, pp. 62–77, Jan. 2011.

[12] F. Zong, M. Zeng, Z. He, and Y. Yuan, "Bus-car mode identification: Traffic condition-based random-forests method," *J. Transp. Eng., A, Syst.*, vol. 146, no. 10, 2020, Art. no. 04020113, doi: 10.1061/JTEPBS.0000442.

[13] M. Scott and S. Y. He, "Modeling constrained destination choice for shopping: A GIS-based time-geographic approach," *J. Transp. Geogr.*, vol. 23, pp. 60–71, Jul. 2012.

[14] D. Helbing and B. Tilch, "Generalized force model of traffic dynamics," *Phys. Rev. E, Stat. Phys. Plasmas Fluids Relat. Interdiscip. Top.*, vol. 58, no. 1, pp. 133–138, Jul. 1998.

[15] M. Treiber, A. Hennecke, and D. Helbing, "Derivation, properties, and simulation of a gas-kinetic-based, nonlocal traffic model," *Phys. Rev. E, Stat. Phys. Plasmas Fluids Relat. Interdiscip. Top.*, vol. 59, no. 1, pp. 239–253, Jan. 1999.

[16] R. Jiang, Q. Wu, and Z. Zhu, "Full velocity difference model for a car-following theory," *Phys. Rev. E, Stat. Phys. Plasmas Fluids Relat. Interdiscip. Top.*, vol. 64, no. 1, pp. 017101–017105, Jun. 2001.

[17] Q. Lin, Y. Zhang, S. Verwer, and J. Wang, "MOHA: A multi-mode hybrid automaton model for learning car-following behaviors," *IEEE Trans. Intell. Transp. Syst.*, vol. 20, no. 2, pp. 790–796, Feb. 2019.

[18] M. Farzaneh and H. Rakha, "Impact of differences in driver-desired speed on steady-state traffic stream behavior," *Transp. Res. Rec., J. Transp. Res. Board*, vol. 1965, no. 1, pp. 142–151, Jan. 2006.

[19] J. Tang, X. Chen, Z. Hu, F. Zong, C. Han, and L. Li, "Traffic flow prediction based on combination of support vector machine and data denoising schemes," *Phys. A, Stat. Mech. Appl.*, vol. 534, Nov. 2019, Art. no. 120642, doi: 10.1016/j.physa.2019.03.007.

[20] Z. Xiaomei and G. Ziyou, "The stability analysis of the full velocity and acceleration velocity model," *Phys. A, Stat. Mech. Appl.*, vol. 375, no. 2, pp. 679–686, Mar. 2007.

[21] H. X. Ge, S. Q. Dai, L. Y. Dong, and Y. Xue, "Stabilization effect of traffic flow in an extended car-following model based on an intelligent transportation system application," *Phys. Rev. E, Stat. Phys. Plasmas Fluids Relat. Interdiscip. Top.*, vol. 70, no. 6, pp. 066134–066140, Dec. 2004.

[22] M. Bando, K. Hasebe, A. Nakayama, A. Shibata, and Y. Sugiyama, "Dynamical model of traffic congestion and numerical simulation," *Phys. Rev. E, Stat. Phys. Plasmas Fluids Relat. Interdiscip. Top.*, vol. 51, pp. 1035–1042, Feb. 1995.

[23] D. Helbing and B. Tilch, "Generalized force model of traffic dynamics," *Phys. Rev. E, Stat. Phys. Plasmas Fluids Relat. Interdiscip. Top.*, vol. 58, no. 1, pp. 133–138, Jul. 1998.

[24] R. Jiang, Q. Wu, and Z. Zhu, "Full velocity difference model for a car-following theory," *Phys. Rev. E, Stat. Phys. Plasmas Fluids Relat. Interdiscip. Top.*, vol. 64, no. 1, pp. 017101–017105, Jun. 2001.

[25] M. Treiber, A. Hennecke, and D. Helbing, "Congested traffic states in empirical observations and microscopic simulations," *Phys. Rev. E, Stat. Phys. Plasmas Fluids Relat. Interdiscip. Top.*, vol. 62, no. 2, pp. 1805–1824, Aug. 2000.
[26] M. Treiber, A. Kesting, and D. Helbing, "Delays, inaccuracies and anticipation in microscopic traffic models," *Phys. A, Stat. Mech. Appl.*, vol. 360, no. 1, pp. 71–88, Jan. 2006.
[27] S. J. Zhu, S. Qu, and Q. X. Shi, "Improvement for intelligent driver model and its application," *Central South Highway Eng.*, vol. 3, pp. 135–139, Jan. 2006.
[28] Z. Li, W. Li, S. Xu, and Y. Qian, "Stability analysis of an extended intelligent driver model and its simulations under open boundary condition," *Phys. A, Stat. Mech. Appl.*, vol. 419, pp. 526–536, Feb. 2015.
[29] M. Treiber, A. Kesting, and D. Helbing, "Understanding widely scattered traffic flows, the capacity drop, and platoons as effects of variance-driven time gaps," *Phys. Rev. E, Stat. Phys. Plasmas Fluids Relat. Interdiscip. Top.*, vol. 74, no. 1, Jul. 2006, Art. no. 016123.
[30] Y. Li, D. Sun, W. Liu, M. Zhang, M. Zhao, X. Liao, and L. Tang, "Modelling and simulation for microscopic traffic flow based on multiple headway, velocity and acceleration difference," *Nonlinear Dyn.*, vol. 66, nos. 1–2, pp. 15–28, 2011.
[31] G. Hong-Xia, C. Yu, and C. Rong-Jun, "A car-following model with considering control signals from front and rear," *Acta Phys. Sinica*, vol. 63, no. 11, Dec. 2014, Art. no. 110504.
[32] D. Yang, "Modelling and analysis of the car-following behaviour considering the following vehicle," Southwest Jiaotong Univ., Chengdu, China, Tech. Rep., 2013, pp. 3–62, vol. 21.
[33] A. Nakayama, Y. Sugiyama, and K. Hasebe, "Effect of looking at the car that follows in an optimal velocity model of traffic flow," *Phys. Rev. E, Stat. Phys. Plasmas Fluids Relat. Interdiscip. Top.*, vol. 65, no. 1, Dec. 2001, Art. no. 016112.
[34] H. X. Ge, H. B. Zhu, and S. Q. Dai, "Effect of looking backward on traffic flow in a cooperative driving car following model," *Eur. Phys. J. B*, vol. 54, no. 4, pp. 503–507, Dec. 2006.
[35] D.-H. Sun, X.-Y. Liao, and G.-H. Peng, "Effect of looking backward on traffic flow in an extended multiple car-following model," *Phys. A, Stat. Mech. Appl.*, vol. 390, no. 4, pp. 631–635, Feb. 2011.
[36] J. Sau, J. Monteil, R. Billot, and N.-E. El Faouzi, "The root locus method: Application to linear stability analysis and design of cooperative car-following models," *Transportmetrica B, Transp. Dyn.*, vol. 2, no. 1, pp. 60–82, Jan. 2014.
[37] P. Guang-Han, "Stabilisation analysis of multiple car-following model in traffic flow," *Chin. Phys. B*, vol. 19, no. 5, May 2010, Art. no. 056401.
[38] H. M. Zhang, "Analyses of the stability and wave properties of a new continuum traffic theory," *Transp. Res. B, Methodol.*, vol. 33, no. 6, pp. 399–415, Aug. 1999.
[39] T.-Q. Tang, H.-J. Huang, Y. Zhang, and X.-Y. Xu, "Stability analysis for traffic flow with perturbations," *Int. J. Mod. Phys. C*, vol. 19, no. 09, pp. 1367–1375, Sep. 2008.
[40] M. Treiber and A. Kesting, *Traffic Flow Dynamics Traffic Flow Dynamics*. Berlin, Germany: Springer, 2013.

FANG ZONG received the B.S. degree in automobile application engineering, and the M.S. and Ph.D. degrees in transportation planning and management from Jilin University, Changchun, China, in 2002, 2005, and 2008, respectively.

She is currently a Professor with Transportation College, Jilin University. She has completed more than 50 research projects totally and obtained seven national invention patents. Her research interests include traffic accident analysis, travel behavior identification with GPS data, traffic simulation, decision making, and intelligent optimization. She has published more than 40 articles in journals and conference proceedings in the above research areas including IET-Intelligent Transportation System and Proceedings, Institution of Civil Engineers-Transport.

Prof. Zong serves as a frequent reviewer for more than ten international journals.

MENG WANG was born in Zaozhuang, Shandong, China, in 1992. He received the B.S. degree in logistics engineering from the Shandong University of Science and Technology, Qingdao, China, in 2011, and the M.S. degree in logistics management from Northeast Forestry University, Harbin, China, in 2019. He is currently pursuing the Ph.D. degree with the Transportation College, Jilin University, China.

His research interests include traffic simulation, image processing, and big data analysis.

MING TANG received the B.S. and M.S. degrees in transportation engineering from the Changsha University of Science and Technology, Changsha, China, in 1999 and 2004, respectively, and the Ph.D. degree from Jilin University, Changchun, in 2010. He is currently an Instructor with Transportation College, Jilin University. His research interests include intelligent transportation and slow traffic system planning.

XIYING LI received the Ph.D. degree in optical engineering from the Beijing Institute of Technology, in 2002. She was the Visiting Scholar with Washington University. She is currently an Associate Professor with the School of Intelligent Systems Engineering, Sun Yat-sen University. Her main research interests include vehicle recognition and tracking, traffic video analysis and understanding, pedestrian detection and recognition, and video big data.

MENG ZENG was born in Shaoyang, Hunan, China, in 1993. She received the B.S. degree in road, bridge and river-crossing engineering and the M.S. degree in traffic engineering from Chang'an University, Xi'an, China, in 2015 and 2018, respectively. She is currently pursuing the Ph.D. degree with Transportation College, Jilin University, China.

Her research interests include travel behavior identification, traffic simulation, and decision making.